

# Photoinduced phase transition in VO<sub>2</sub> nanocrystals: ultrafast control of surface-plasmon resonance

Matteo Rini, Andrea Cavalleri, and Robert W. Schoenlein

Materials Sciences Division, Lawrence Berkeley National Laboratory, 1 Cyclotron Road, Berkeley, California 94720

René López, Leonard C. Feldman, and Richard F. Haglund, Jr.

Department of Physics and Astronomy, Vanderbilt University, 6301 Stevenson, Nashville, Tennessee 37235

Lynn A. Boatner and Tony E. Haynes

Condensed Matter Sciences Division, Oak Ridge National Laboratory, Oak Ridge, Tennessee 37831

Received July 29, 2004

We study the ultrafast insulator-to-metal transition in nanoparticles of VO<sub>2</sub>, obtained by ion implantation and self-assembly in silica. The nonmagnetic, strongly correlated compound VO<sub>2</sub> undergoes a reversible phase transition, which can be photoinduced on an ultrafast time scale. In the nanoparticles, prompt formation of the metallic state results in the appearance of surface-plasmon resonance. We achieve large, ultrafast enhancement of optical absorption in the near-infrared spectral region that encompasses the wavelength range for optical-fiber communications. One can further tailor the response of the nanoparticles by controlling their shape. © 2005 Optical Society of America

OCIS codes: 320.7130, 160.4670, 320.7150, 160.4760, 300.6500.

The phase transitions exhibited by strongly correlated compounds are often associated with large changes in the electrical, optical, and magnetic properties of these compounds. Strong interactions among the many degrees of freedom of the system create complex free energy surfaces and multiple isoenergetic ground states. One way to control competition among phases is by light illumination, which can initiate phase transitions at moderate intensities<sup>1</sup> or drive large optical nonlinearities.<sup>2</sup> This behavior is potentially conducive to new strategies for ultrafast optical switching applications.<sup>2,3</sup> However, compatibility with existing technologies, operating temperatures, and wavelengths is often a critical limitation for applications of bulk materials. The design of nanometer-scale structures can be used to adapt desirable properties of extended solids to specific applications. Here we study how dielectric confinement and particle shape affect the change in optical properties across the room-temperature, photoinduced insulator-to-metal phase transition in nanoparticles of VO<sub>2</sub> embedded in a silica matrix. We have found that confinement to the nanometer scale greatly enhances the differential absorption of VO<sub>2</sub> in the optical telecommunications window.

VO<sub>2</sub> is a nonmagnetic, strongly correlated compound that undergoes a reversible phase transition between a monoclinic insulator and a rutile metal at a critical temperature  $T_c = 340$  K.<sup>4</sup> The phase transformation of the bulk oxide is accompanied by large changes in the optical transmission properties<sup>5</sup> and can be induced on a femtosecond time scale by ultrashort laser pulses.<sup>6</sup> Time-resolved optical and x-ray diffraction experiments with bulk VO<sub>2</sub> have clarified some of the fundamental aspects of its ultrafast response.<sup>6,7</sup> Prompt photoinjection of holes into

the correlated valence band of the room-temperature insulator triggers nonthermal rearrangement in both atomic and electronic structures within a time scale of 70 fs.<sup>8</sup> Recovery of the insulating phase takes place within tens of nanoseconds via thermal diffusion.<sup>6</sup>

The VO<sub>2</sub> nanoparticles studied here are grown by ion implantation and self-assembly in silica.<sup>9</sup> Their size and shape are controlled by variation of the annealing time.<sup>10</sup> Figure 1 compares the thermally induced changes of absorbance ( $\Delta\alpha$ ) for a VO<sub>2</sub> film and for a layer of spherical nanoparticles of comparable depth and 10% volume filling. In the thin films, absorption in the metallic phase is enhanced by the collapse of the 0.67-eV optical bandgap at long wavelengths and by the appearance of the plasma edge near 800 nm.

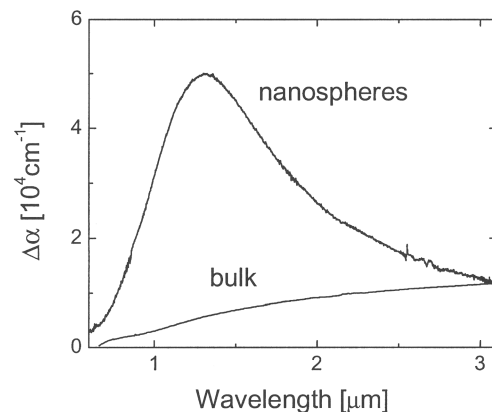


Fig. 1. Change of absorbance in VO<sub>2</sub> across the temperature-driven phase transition for thin-film and spherical nanoparticles as derived from steady-state absorption measurement in the low- and high-temperature phases. The VO<sub>2</sub> volume filling for nanospheres is approximately 10% in a single 100-nm layer.

In the nanoparticles a strong surface-plasmon resonance that is absent in the bulk dominates the optical response. This resonance is due to collective oscillations of the electron plasma, which can directly couple to light in a dielectrically confined geometry.<sup>11</sup> The large absorption coefficient at the surface-plasmon frequency can be calculated from the classical Mie formula for the polarizability of a spherical particle, for particle sizes much smaller than the wavelength of light. In the absence of damping, the polarizability diverges when the real part of the dielectric constant equals  $-2\epsilon_m$ , where  $\epsilon_m$  is the dielectric constant of the surrounding medium. This singularity, which is relaxed in the presence of damping, can be observed only when the nanoparticles are in the metallic phase, in which the real part of the dielectric constant is negative.

The ultrafast photoinduced response in the near and mid infrared is investigated by femtosecond pump-probe spectroscopy.<sup>12</sup> The transient  $\Delta T/T$  spectrum measured 200 fs after 800-nm excitation is shown in Fig. 2(a) for spherical particles. The agreement between time-resolved data and static spectra of the thermally induced phase transition is evidence that the VO<sub>2</sub> nanoparticles have reached the metallic phase immediately after excitation. This result is consistent with previous observations in bulk samples.<sup>8</sup> The photoinduced transmission drop appears at all wavelengths within the experimental time resolution (<150 fs), without significant dynamics at later times. Figure 2(b) shows the pump-probe signal as a function of pulse delay measured at 1.55 and 2.5  $\mu\text{m}$ . Optical transparency recovers on a nanosecond time scale, with the return to the insulating phase. The ultrafast transmission changes exhibit a well-defined fluence threshold of  $\sim 300 \mu\text{J}/\text{cm}^2$  as well as saturation effects, as expected from a photoinduced phase transition: Above threshold, the dielectric properties of the nanoparticles settle to the value that is characteristic of the new phase, independently of the excitation fluence.

The dependence of the plasmon resonance on the size and shape of the nanoparticles<sup>11</sup> can be exploited to further tailor the spectral response. Relative transmission changes ( $\Delta T/T$ ), measured 200 fs after excitation of the room-temperature insulator, are displayed in Fig. 3 for samples with mean aspect ratios that vary from 1 (spherical particles) to 3.5. For a constant amount of VO<sub>2</sub>, the transmission changes in the longer-wavelength range scale with increasing aspect ratio. The dependence on wavelength and shape of the  $\Delta T/T$  spectra is well described by Mie scattering theory,<sup>11</sup> as shown by the solid curves of Fig. 3.<sup>13</sup> According to Mie theory, the resonance condition for nonspherical particles depends on the particles' orientation relative to the electric field's polarization. For ellipsoidal nanoparticles with their major axes parallel to the plane of incidence, Mie theory predicts absorption features at longer wavelengths for polarization parallel to the major axis. Thus the continuous angular distribution of randomly oriented rods in our samples results in overall broadening of the absorption spectrum toward longer wavelengths.

Remarkable features of the switching behavior investigated here include room-temperature operation, compatibility with fiber-optic environment,<sup>10</sup> and high efficiency at telecommunication wavelengths (1.3–1.5  $\mu\text{m}$ ). Moreover, the 300- $\mu\text{J}/\text{cm}^2$  threshold for the photoinduced phase transition is equivalent to a 150-pJ pulse for a typical 50- $\mu\text{m}^2$  mode size in a single-mode fiber, making such schemes attractive for real-world applications. In the particles with the highest aspect ratio, we observed a switching efficiency of  $\sim 25\%$  at 1.55  $\mu\text{m}$  over a propagation length of less than 100 nm and for a VO<sub>2</sub> filling factor of less than 10%. One could straightforwardly achieve higher switching contrasts by increasing areal filling factors or interaction length. Clearly, the nanosecond lifetime of the metallic state limits the suitability of VO<sub>2</sub> for all-optical switching at high bit rates. However, similarly large optical nonlinearities<sup>2</sup> and optical switching with intrinsic subpicosecond recovery times<sup>3</sup> have been observed in bulk samples of other transition-metal oxides, making them attractive for similar nanoscale design strategies. Further, the capability

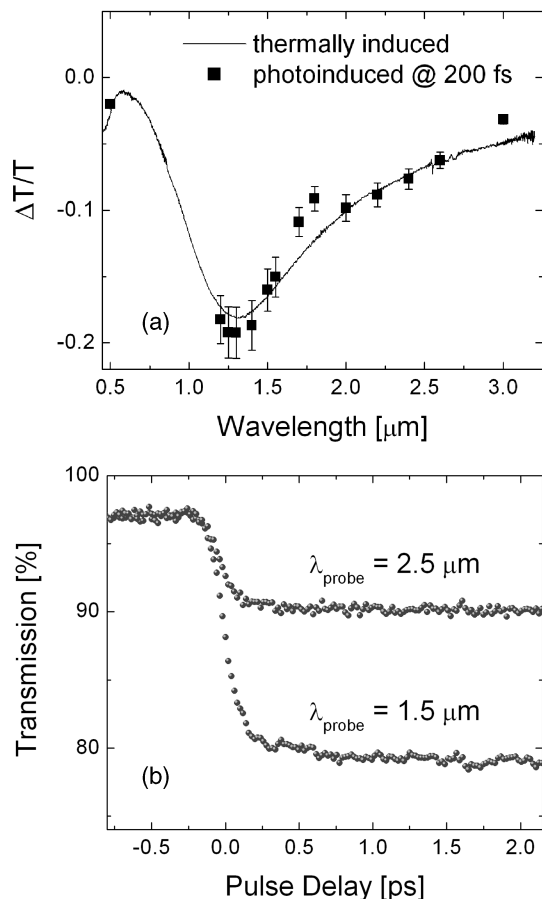


Fig. 2. (a) Relative change of transmission across the phase transition for the VO<sub>2</sub> nanospheres. ( $\Delta T$ , change of transmission in the presence of the pump;  $T$ , sample transmission). The thermally induced curve was derived from spectra measured at room temperature (VO<sub>2</sub> in the insulating phase) and at 373 K (VO<sub>2</sub> in the metallic phase). The photoinduced wave was measured at a delay of 200 fs after photoexcitation. (b) Pump-probe signal as a function of pulse delay measured at 1.55 and 2.5  $\mu\text{m}$ .

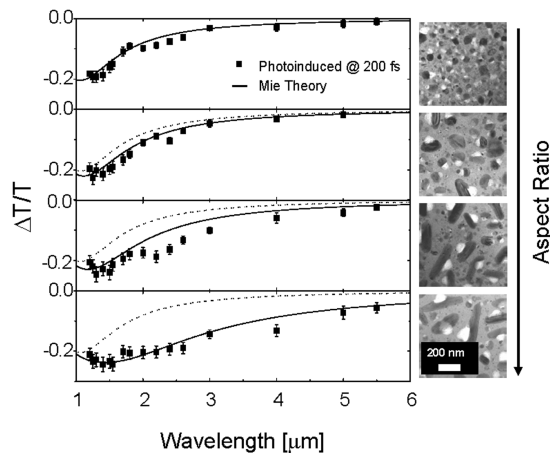


Fig. 3. Relative change of transmission as a function of wavelength for several aspect ratios (top to bottom: 1, 1.5, 2, 3.5) as obtained by varying the annealing time (3, 7, 10, and 45 min, respectively). Squares, measured at a delay of 200 fs after photoexcitation; solid curves, calculations based on Mie scattering theory. As a comparison, dashed curves show the prediction of Mie theory for spherical particles (aspect ratio, 1; the same as in the topmost figure). Representative TEM pictures of the corresponding samples are shown at the right.

of addressing the conducting states of nanoparticles, individually or within ensembles, may be useful for nanophotonic devices that rely on collective plasmon modes for the transport of electromagnetic energy.<sup>14</sup>

In summary, we have shown that (1) photoexcitation of the VO<sub>2</sub> nanoparticles results in the formation of the metallic phase within less than 150 fs; (2) as the particles reach the metallic phase, the absorption spectrum exhibits a surface-plasmon resonance near telecommunication wavelengths; (3) the dependence of the resonance on the shape of the nanoparticles makes it possible to tailor the spectral responses of the nanoparticles. Most remarkably, our results demonstrate that nanoscale phenomena can lead to enabling strategies for the integration of strongly correlated solids into ultrafast optical devices.

Research at the Lawrence Berkeley National Laboratory was supported by the Director, Office of Science, Office of Basic Energy Sciences, Division of Materials Sciences and Engineering, U.S. Department of Energy, under contract DE-AC03-76SF00098. Research at Vanderbilt University was supported by the Office of Science, U.S. Department of Energy (DE-FG02-01-ER45916), and by the National Science Foundation (DMR0210785). Research at the Oak Ridge National Laboratory, managed by UT-Battelle, LLC, for the U.S. Department of Energy under contract DE-AC05-00OR22725, was supported by

the Laboratory Directed Research and Development Program. M. Rini's e-mail address is mrini@lbl.gov.

## References

1. K. Miyano, T. Tanaka, Y. Tomioka, and Y. Tokura, *Phys. Rev. Lett.* **78**, 4257 (1997).
2. T. Ogasawara, M. Ashida, N. Motoyama, H. Eisaki, S. Uchida, Y. Tokura, H. Ghosh, A. Shukla, S. Mazumdar, and M. Kuwata-Gonokami, *Phys. Rev. Lett.* **85**, 2204 (2000).
3. S. Iwai, M. Ono, A. Maeda, H. Matsuzaki, H. Kishida, H. Okamoto, and Y. Tokura, *Phys. Rev. Lett.* **91**, 057401 (2003).
4. F. J. Morin, *Phys. Rev. Lett.* **3**, 34 (1959).
5. H. W. Verleur, A. S. Barker, Jr., and C. N. Berglund, *Phys. Rev.* **172**, 788 (1968).
6. M. F. Becker, A. B. Buckman, R. M. Walsler, T. Lépine, P. Georges, and A. Brun, *J. Appl. Phys.* **79**, 2404 (1994).
7. A. Cavalleri, Cs. Tóth, C. W. Siders, J. A. Squier, F. Rákai, P. Forget, and J. C. Kieffer, *Phys. Rev. Lett.* **87**, 237401 (2001).
8. A. Cavalleri, Th. Dekorsy, H. H. Chong, J. C. Kieffer, and R. W. Schoenlein, *Phys. Rev. B* **70**, 161102 (2004).
9. Samples are prepared by implantation of vanadium ions ( $1.5 \times 10^{17}$  V ions/cm<sup>2</sup> at 150 keV) and oxygen ions ( $3.0 \times 10^{17}$  O ions/cm<sup>2</sup> at 55 keV) at equal depths of 120 nm into an amorphous SiO<sub>2</sub> substrate and then annealing in an argon atmosphere at 1000 °C. Depending on the annealing time, the mean radius of the nanoparticles varies from 40 to 80 nm. See R. Lopez, L. A. Boatner, T. E. Haynes, L. C. Feldman, and R. F. Haglund, Jr., *J. Appl. Phys.* **92**, 4031 (2002).
10. R. Lopez, T. E. Haynes, L. A. Boatner, L. C. Feldman, and R. F. Haglund, Jr., *Opt. Lett.* **27**, 1327 (2002).
11. H. C. van de Hulst, *Light Scattering by Small Particles* (Dover, New York, 1981).
12. The experimental setup is based on a 1-kHz Ti:sapphire laser. Pump pulses at 800 nm have 1–3-μJ energy and durations below 50 fs. Near-infrared pulses are obtained from an optical parametric amplifier (signal, 1.1–1.6 μm; idler, 1.6–2.6 μm). Mid-infrared 2.8–6 μm pulses are generated by difference-frequency mixing in GaSe of signal and idler pulses. The time resolution varies from 100 to 150 fs, with increasing values from high to low frequencies. As the phase transition is fully reversible, the sample is not moved from shot to shot.
13. The particles are considered perfect ellipsoids placed in a homogeneous electromagnetic field with their major axes perpendicular to the direction of light propagation and a random in-plane orientation. Inhomogeneous effects that are due to a size and aspect ratio distribution of the nanorods are neglected, as are interparticle coupling mechanisms. The complex dielectric function of the high-temperature metallic VO<sub>2</sub> is employed.<sup>8</sup>
14. S. A. Maier, P. G. Kik, H. A. Atwater, S. Meltzer, E. Harel, B. E. Koel, and A. A. G. Requicha, *Nature Mater.* **2**, 229 (2003).